Supplementary Information for
Experimental Realization of a One-Atom Laser in the Regime of Strong Coupling

J. McKeever, A. Boca, A. D. Boozer, J. R. Buck, and H. J. Kimble

Norman Bridge Laboratory of Physics 12-33, California Institute of Technology, Pasadena, CA 91125

(Dated: September 11, 2003)

Additional information is provided about the theoretical background and data analysis presented in our paper, Ref. [1].

I. INTRODUCTION

Although a number of theoretical treatments related to a one-atom laser have appeared in the literature [2–12], this prior work has not been specific to the parameter range of our experiment as reported in Ref. [1]. A principal purpose of this *Supplementary Information* is to present a brief description of the relationship of the operating regime of our experiment to that of more conventional laser systems. We establish this connection in Section *II* by way of a simplified four-state model that captures the essential features of the operation of our one-atom laser in a domain of strong coupling. Results from semiclassical and quantum solutions for a one-atom laser based upon this four-state model are presented in turn. This brief synopsis is elaborated in much more detail in Ref. [13], including an expanded model that incorporates the relevant Zeeman substructure for the Cesium atom (32 atomic states), two modes of the cavity with orthogonal polarizations, and a simple model to account for the polarization gradients of the $\Omega_{3,4}$ fields. Ref. [13] also provides a comparison of the results from quantum jumps simulations based upon this expanded model with the measurements in Figure 3 for $\bar{n}$ versus normalized pump intensity x and in Figure 4 for the intensity correlation function $g^{(2)}(\tau)$.

The second purpose of this *Supplementary Information* is to present the actual coincidence data that are the basis of Fig. 4 in our manuscript [1], which we do in Section *III*. We also describe the procedure employed for obtaining the normalized intensity correlation function $g^{(2)}(\tau)$ from these data.

II. COMPARISON OF SEMICLASSICAL AND QUANTUM THEORIES FOR A FOUR-STATE ATOM

As noted in our paper Ref. [1], a one-atom laser operated in a regime of strong coupling with $(N_0, n_0) \ll 1$ will evidence qualitatively different characteristics than those of more familiar conventional lasers. The question then arises as how best to identify a laser in this new regime, with diverse criteria suggested and analyzed in prior work on one-atom lasers [2–12]. The perspective that we adopt here is to trace the lineage of our one-atom laser from a conventional regime continuously into the domain of strong coupling. We do this by considering a scenario where an atom is placed inside a cavity which undergoes a transformation from very large to very small mode volume. The cavity length l is reduced such that the cross-sectional area of the cavity mode at the position of the atom and the mirror reflectivity are both held constant. Since $g_0 \propto l^{-1/2}$ and $\kappa \propto l^{-1}$, $N_0 = \frac{2\kappa\gamma}{g_0^2}$ remains constant independent of l. On the other hand, the saturation photon number $n_0 = \frac{\gamma^2}{2g_0^2} \propto l$ decreases, so that the electric field per photon $E_1 \propto \frac{1}{\sqrt{n_0}}$ increases. Hence the

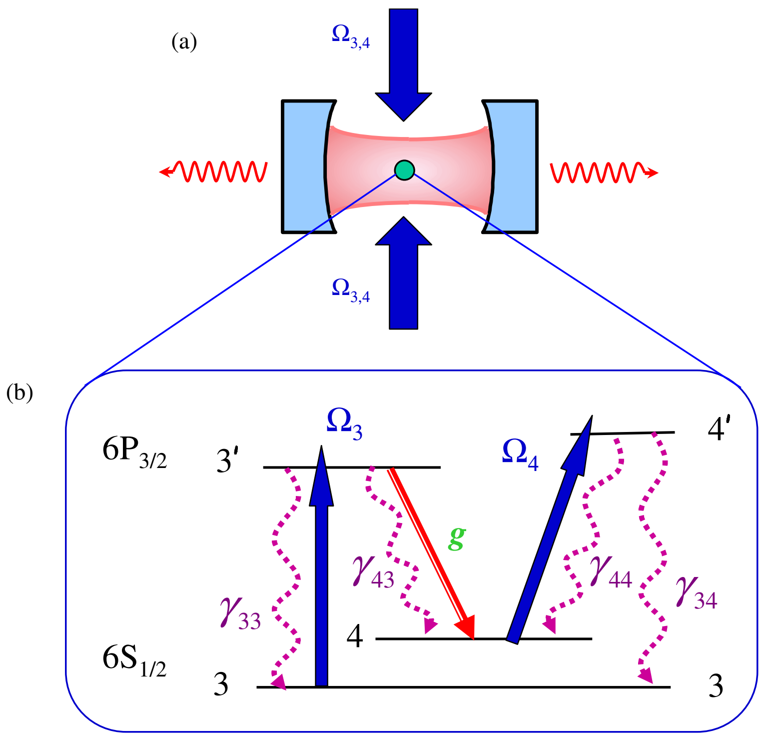

FIG. A: Illustration of a one-atom laser. (a) The atom is located in a high-Q optical cavity of decay rate κ, and is driven by the fields $\Omega_{3,4}$. (b) Inset of the atomic level scheme relevent to our experiment with the $6S_{1/2} \leftrightarrow 6P_{3/2}$ transition in atomic Cesium. The "lasing" transition is from the excited level $F' = 3'$ to the ground level $F = 4$. Pumping of the excited $3'$ level is by way of coherent excitation from a laser with Rabi frequency Ω_3. Effective decay from the ground 4 level is provided by the combination of a second field with Rabi frequency Ω_4 and spontaneous decay $4' \rightarrow 3$. The partial decay rates shown are appropriate to radiative decay of the levels $6P_{3/2}, F' = 3', 4' \rightarrow 6S_{1/2}, F = 3, 4$ with $\gamma = 2\pi \times 2.6$ MHz (i.e., a radiative lifetime $\tau = 1/2\gamma = 30.6$ ns) and are as follows: $(\gamma_{33}, \gamma_{43}, \gamma_{44}, \gamma_{34}) = (\frac{3}{4}, \frac{1}{4}, \frac{7}{12}, \frac{5}{12})\gamma$, where γ_{ij} is the (amplitude) decay rate from level j to level i. The cavity (field) decay rate κ is measured to be $\kappa = 2\pi \times 4.2$ MHz. The rate of coherent coupling g_{43} for the the $3' \leftrightarrow 4$ transition (i.e., $6P_{3/2}, F' = 3' \leftrightarrow 6S_{1/2}, F = 4$) is determined from the known cavity geometry (waist and length) and the decay rate γ, and is found to be $g_{43} = 2\pi \times 16$ MHz based upon the effective dipole moment for the transition.

simple prescription of "shrinking" the cavity leads inevitably to a regime for which single-photon processes become dominant, and for which predictions from the conventional laser theory and the full quantum analysis diverge.

For a four-state model based upon Fig. A, it is straightforward to derive equations of motion for expectation values of atom and field operators. The conventional semiclassical theory is obtained from the factorization $\langle \hat{\sigma}_{ij}(t)\hat{a}(t)\rangle = \langle \hat{\sigma}_{ij}(t)\rangle\langle \hat{a}(t)\rangle$, where $\hat{\sigma}_{ij} = |i\rangle\langle j|$ are the atomic projection operators for the set of states (i, j) and $\hat{a}$ is the annihilation operator for the intracavity field. The steady-state solution $\alpha \equiv \langle \hat{a}\rangle_{ss}$ to these semiclassical equations is plotted in Fig. B for parameters relevant to our experiment (i.e., same values of (n_0, N_0) and of atomic decay rates) and exhibits a clearly defined laser threshold. Around this threshold, familiar characteristics for conventional lasers are found, including population inversion (see Ref. [13]). In these calculations, we used our experimental value for the cooperativity parameter $C_1 = 1/N_0 \simeq 12$. Indeed, the condition $C_1 \gg 1$ is required to observe threshold behavior for one atom pumped inside the resonator.

To obtain a fully quantum description for the four-state model based upon Fig. A, we carry out numerical solutions of the master equation for the density operator $\hat{\rho}$ for atom and field (see Refs.

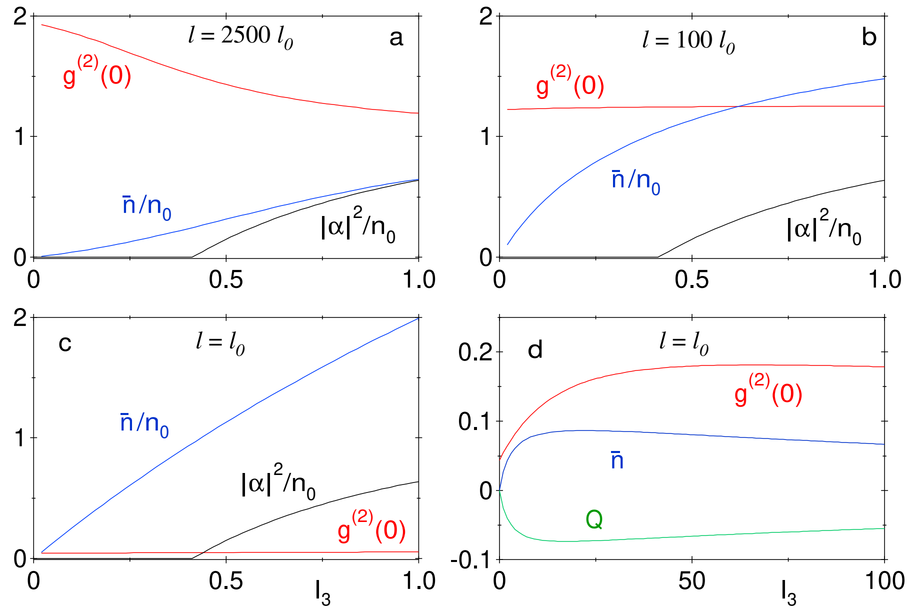

FIG. B: The mean intracavity photon number $\bar{n}/n_0$ (blue) and normalized intensity correlation function $g^{(2)}(0)$ (red) are plotted as functions of pump intensity $I_3 = (\Omega_3/2\gamma)^2$ in (a)-(d). In (a)-(c), the cavity length is made progressively shorter ($2500l_0$, $100l_0$, l_0), where $l_0 = 42.2$ μm is the length of our actual cavity. The corresponding saturation photon numbers are (33.0, 1.32, 0.013). $\bar{n}/n_0$ and $g^{(2)}(0)$ are calculated from the quantum theory for the four-state system in Fig. A, while $|\alpha|^2/n_0$ given by the black curve is from the semiclassical theory. (d) $\bar{n}$ (blue), $g^{(2)}(0)$ (red), and the Mandel Q parameter (green) shown over an extended range of pump intensity I_3 for $l = l_0$. In all cases, $I_4 = (\Omega_4/2\gamma)^2 = 2$, the $3 \to 4'$ and $4 \to 4'$ transitions are driven on resonance, and the cavity detuning $\omega_{CA} = 0$. Other parameters are as given in the caption of Fig. A.

[13, 14]). These solutions can then be employed to investigate the passage from the semiclassical regime to the quantum domain. An example relevant to our experiment is illustrated by the series of curves shown in Fig. B for decreasing cavity length. Clearly, a large cavity volume with $l \gg l_0$ brings us closer to the domain of conventional lasers, as evidenced in Fig. B(a) for $l = 2500l_0$. The laser output curve $\bar{n}/n_0$ versus pump intensity I_3 is to be compared to the semiclassical calculation $|\alpha|^2/n_0$. As for the normalized intensity correlation function $g^{(2)}(0)$ of Fig. B(a), recall that a conventional laser generates an output with Gaussian statistics $g^{(2)}(0) = 2$ below threshold and passes smoothly to light that approximates a coherent state with $g^{(2)}(0) = 1$ as the pump increases through threshold [15, 16]. Moreover, as documented in Ref. [13], for large l the Mandel Q parameter exhibits two maxima as a function of I_3, one around the conventional threshold and one for large pump values [7, 10, 17], which gradually develop into a single broad minimum with decreasing l. In all cases, $\bar{n}$, $g^{(2)}$, and Q, as well as the various atomic populations, display pronounced functional dependencies on the pump level I_3 that require a self-consistent treatment of atom and cavity field, here in the fully quantum regime as opposed to the limit of large (N_0, n_0) in conventional laser theories.

Since N_0 remains constant independent of l and because the semiclassical solution $|\alpha|^2/n_0$ is independent of n_0, the increasing disparity between the functions shown in (a)-(c) in Fig. B for decreasing l indicates the continuous passage away from the domain of conventional laser operation and into a regime of strong coupling where various nonclassical features emerge (e.g., $g^{(2)}(0) < 1$), as predicted in prior treatments of one-atom lasers [2, 4–7, 9–12]. Figure B(d) provides a global perspective of some of these characteristics over a wider range of the pump intensity I_3 for $l = l_0$

relevant to our experiment. The input-output relationship $\bar{n}$ versus I_3 has several key features to be compared with experimental results presented in Ref. [1], namely the immediate onset of emission ("thresholdless" behavior), and the saturation and eventual quenching of the output. The saturation can be attributed to the recycling process being limited by the atomic decay rates, whereas the output reduction at high I_3 is possibly due to the splitting of the pumped excited state $F' = 3'$ by the Autler-Townes effect, although this is still under investigation.

III. PHOTON STATISTICS INFERRED FROM PHOTOELECTRIC COUNTS

In this section, we present the coincidence data that are the basis of Fig. 4 in our paper [1]. Significantly, the nonclassical nature of the light emitted from the atom-cavity system is directly exhibited by these data. We then briefly describe the procedure followed in determining the normalized intensity correlation function $g^{(2)}(\tau)$ from these data.

As illustrated in Fig. 1 of our Ref. [1], the light emitted by the TEM_{00} mode of the cavity is split into two beams that illuminate the two single-photon detectors $D_{1,2}$ (avalanche photodiodes). Each photoelectric pulse from $D_{1,2}$ is stamped with its time of detection (with $\delta = 1$ ns resolution) and then stored. We collect these arrival time records from several thousand trapping events to construct a correlation function. The first step is to convert each of these records to a pair of lists $(a_1^{(r)}, \cdots, a_N^{(r)})$ and $(b_1^{(r)}, \cdots, b_N^{(r)})$ for detectors D_1 and D_2, respectively, where the k^{th} entry of each list is 1 if a photoelectric event was recorded by the detector in time interval $[(k-1)\delta, k\delta]$ and 0 otherwise. The correlation function $n_r(k\delta)$ for the r^{th} atom is then

$$n_r(k\delta) = \sum_j a_j^{(r)} b_{j+k}^{(r)} \ . \tag{1}$$

We sum up all of these correlation functions to get a total $n(\tau) = \sum_r n_r(\tau)$. For the plots in Fig. C, $n(\tau)$ has been convolved with a $\sigma = 5$ ns Gaussian function for the purpose of smoothing the traces.

From Fig. C without further analysis, we observe that $n(0) < n(\tau)$, which provides direct evidence for the explicitly quantum mechanical character of the emitted light [15]. The field from our atom-cavity system exhibits photon antibunching, so that the associated state of the field cannot be described by a Glauber-Sudarshan phase-space function that is positive definite.

Beyond these statements, the normalized intensity correlation function $g^{(2)}(\tau)$ [15] is related to the coincidence data displayed in Fig. C by the following relation:

$$n(\tau) = T\delta(R_1 + \gamma_1)(R_2 + \gamma_2)[1 + (1 + \gamma_a/R_a)^{-1}(1 + \gamma_b/R_b)^{-1}(g^{(2)}(\tau) - 1)] \ . \tag{2}$$

Here $T = \sum_r t_r$, where t_r is the amount of time atom r spent in the cavity, $R_{1,2}$ is counting rate from detector $D_{1,2}$ due to light emitted by the atom (typically $R_{1,2} \sim 5$ kHz from each detector), and $\gamma_{1,2} \sim 500$ Hz is the detector $D_{1,2}$ background counting rate. Note that these various quantities are determined directly for each atom from observations such as presented in Fig. 2 of our paper [1].

---

[1] J. McKeever, A. Boca, A. D. Boozer, J. R. Buck, and H. J. Kimble, A One-Atom Laser in a Regime of Strong Coupling, *Nature* **425**, 268 (18 September, 2003).

[2] Mu, Y. & Savage, C. M. One-atom lasers. *Phys. Rev. A* **46**, 5944-5954 (1992).

[3] Ginzel, C., Briegel, H.-J., Martini, U., Englert, B.-G. & Schenzle, A. Quantum optical master equations: The one-atom laser. *Phys. Rev. A* **48**, 732-738 (1993).

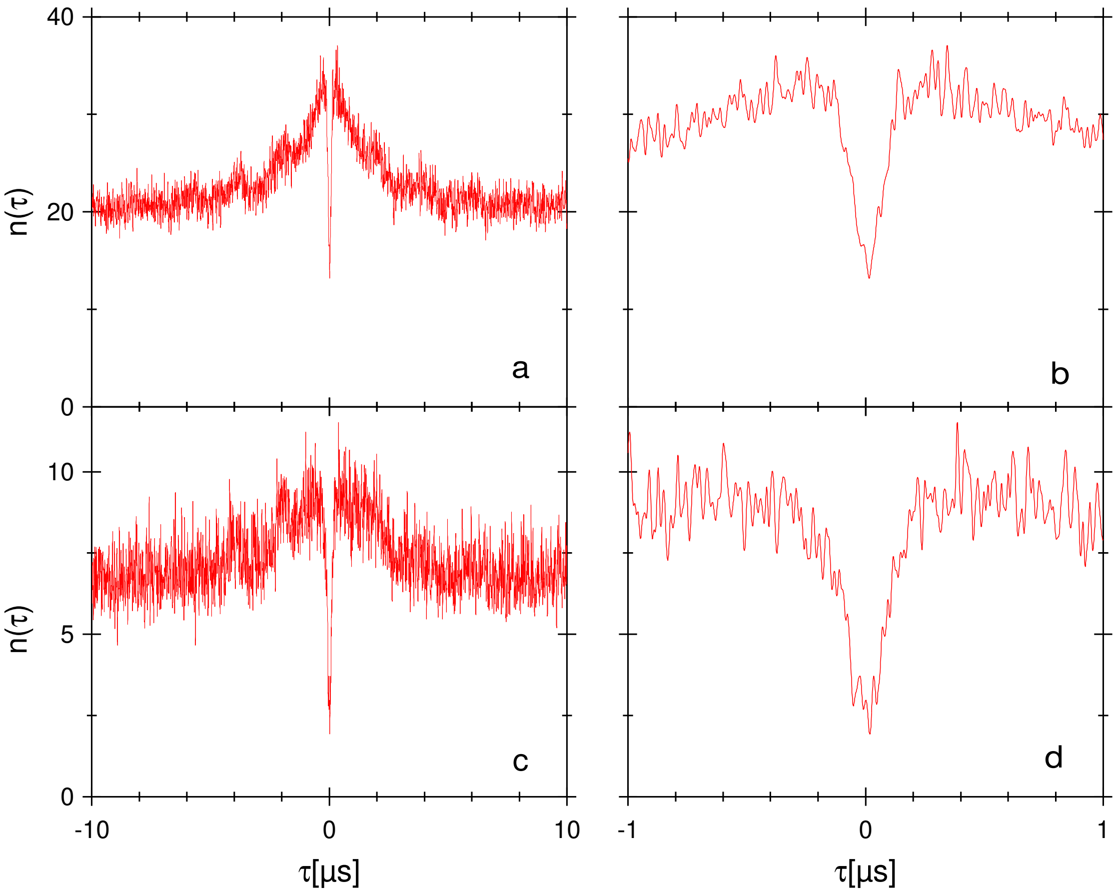

FIG. C: Coincidence counts $n(\tau)$ versus time offset τ obtained from the recorded photoelectric events at detectors $D_{1,2}$. These data were used to obtain $g^{(2)}(\tau)$ in Fig. 4 of our paper [1].

[4] Pellizzari, T. & Ritsch, H. Preparation of stationary Fock states in a one-atom Raman laser. *Phys. Rev. Lett.* **72**, 3973-3976 (1994).

[5] Pellizzari, T. & Ritsch, H. Photon statistics of the three-level one-atom laser. *J. Mod. Opt.* **41**, 609-623 (1994).

[6] Horak, P., Gheri, K. M. & Ritsch, H. Quantum dynamics of a single-atom cascade laser. *Phys. Rev. A* **51**, 3257-3266 (1995).

[7] Meyer, G. M., Briegel, H.-J. & Walther, H. Ion-trap laser. *Europhys. Lett.* **37**, 317-322 (1997).

[8] Löffler, M., Meyer, G. M., & Walther, H. Spectral properties of the one-atom laser. *Phys. Rev. A* **55**, 3923-3930 (1997).

[9] Meyer, G. M., Löffler, M. & Walther, H. Spectrum of the ion-trap laser. *Phys. Rev. A* **56**, R1099-R1102 (1997).

[10] Meyer, G. M. & Briegel, H.-J. Pump-operator treatment of the ion-trap laser. *Phys. Rev. A* **58**, 3210-3220 (1998).

[11] Jones, B., Ghose, S., Clemens, J. P., Rice, P. R. & Pedrotti, L. M. Photon statistics of a single atom laser. *Phys. Rev. A* **60**, 3267-3275 (1999).

[12] Kilin, S. Ya. & Karlovich, T. B. Single-atom laser: Coherent and nonclassical effects in the regime of a strong atom-field correlation. *JETP* **95**, 805-819 (2002).

[13] Boozer, A. D., Boca, A., Buck, J. R., McKeever, J. and Kimble, H. J., Comparison of Theory and Experiment for a One-Atom Laser in a Regime of Strong Coupling, submitted to Phys. Rev. A (2003); preprint available at *http://lanl.arxiv.org/archive/quant-ph*.

[14] Tan, S. M. A computational toolbox for quantum and atomic optics. *J. Opt. B: Quantum Semiclass. Opt.* **1**, 424-432 (1999).

[15] *Optical Coherence and Quantum Optics*, L. Mandel and E. Wolf (Cambridge University Press, 1995).
[16] Gardiner, C. W. & Zoller, P. *Quantum Noise* (Springer-Verlag, Berlin, 2000).
[17] Rice, P. R. & Carmichael, H. J. Photon statistics of a cavity-QED laser: A comment on the laser-phase-transition analogy. *Phys. Rev. A* **50**, 4318-4329 (1994).